

## Supplementary information

### Local atomic and electronic structure in the $\text{Li}_x\text{VPO}_4(\text{F},\text{O})$ Tavorite-type materials from Solid State NMR combined with DFT calculations

T. Bamine<sup>a,b</sup>, E. Boivin<sup>a,b,d</sup>, C. Masquelier<sup>b,c,d</sup>, L. Croguennec<sup>a,b,c</sup>, Elodie Salager<sup>b,e</sup>, and

D. Carlier<sup>a,b,c\*</sup>

<sup>a</sup> CNRS, Univ. Bordeaux, Bordeaux INP, ICMCB UMR 5026, F-33600 Pessac, France

<sup>b</sup> RS2E, Réseau Français sur le Stockage Electrochimique de l'Energie, FR CNRS 3459,  
F-80039 Amiens Cedex 1, France

<sup>c</sup> ALISTORE-ERI, FR3104, 80039 Amiens cedex, France

<sup>d</sup> Laboratoire de Réactivité et de Chimie des Solides, CNRS-UMR#7314,  
Université de Picardie Jules Verne, F-80039 Amiens Cedex 1, France

<sup>e</sup> CNRS, CEMHTI UPR 3079, Université d'Orléans, Orléans, France

		Exp. Shift (ppm)	Calculated Fermi contact Shift (ppm)	
			GGA	GGA+U (4eV)
LiVPO <sub>4</sub> F	<sup>7</sup> Li	115	130	116
	<sup>31</sup> P	3871	6900	3450
	<sup>19</sup> F	-1500	-630	-140
LiVPO <sub>4</sub> O	<sup>7</sup> Li(1)	79	110	44
	<sup>7</sup> Li(2)		105	40
	<sup>31</sup> P(1)	1613	2815	1834
	<sup>31</sup> P(2)	1441	2600	1577

**Figure S1:** Calculated Fermi contact shifts for <sup>7</sup>Li, <sup>31</sup>P and <sup>19</sup>F in LiVPO<sub>4</sub>F and <sup>7</sup>Li and <sup>31</sup>P in LiVPO<sub>4</sub>O compared to experimental ones while spinning at 30 kHz (T~320 K). Calculations were done using GGA and GGA+U approaches. In our previous study on LiVPO<sub>4</sub>F, several values were used for the U term: as 4eV led to good agreement between calculated and experimental shifts it has been chosen in the previous study ref [1]. Further details concerning the Fermi contact shifts calculations using this method can be found in ref [1-2]. Overall, a localization of the electron on the Vanadium d orbital generated by the U term, induces a weaker spin transfer on the adjacent nuclei and thus a weaker computed Fermi contact shift. It was already discussed in our previous studies [3-4].

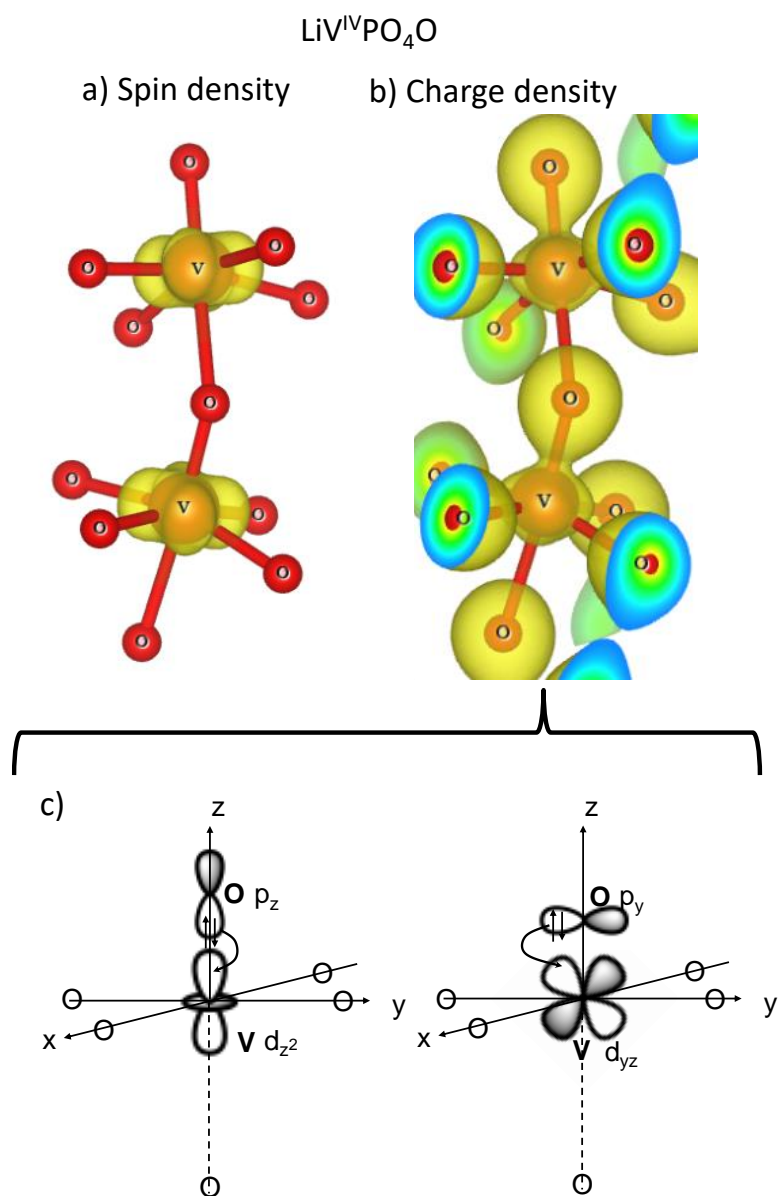


**Figure S2:** The peculiar electronic structure of  $\text{V}^{4+}$  ions involved in the vanadyl ( $\text{V}=\text{O}$ ) bonds in  $\text{LiVPO}_4\text{O}$ . (a) 3D spin density map showing that the  $d_{xy}$  orbital perpendicular to the short  $\text{V}=\text{O}$  bond is carrying the spin. (b) 3D charge density map showing the strong covalency of the  $\text{V}=\text{O}$  bond and (c) the theoretical formation of this double bond involving the  $d_{z^2}$  and the  $d_{yz}$  (or  $d_{xz}$ ) orbitals.

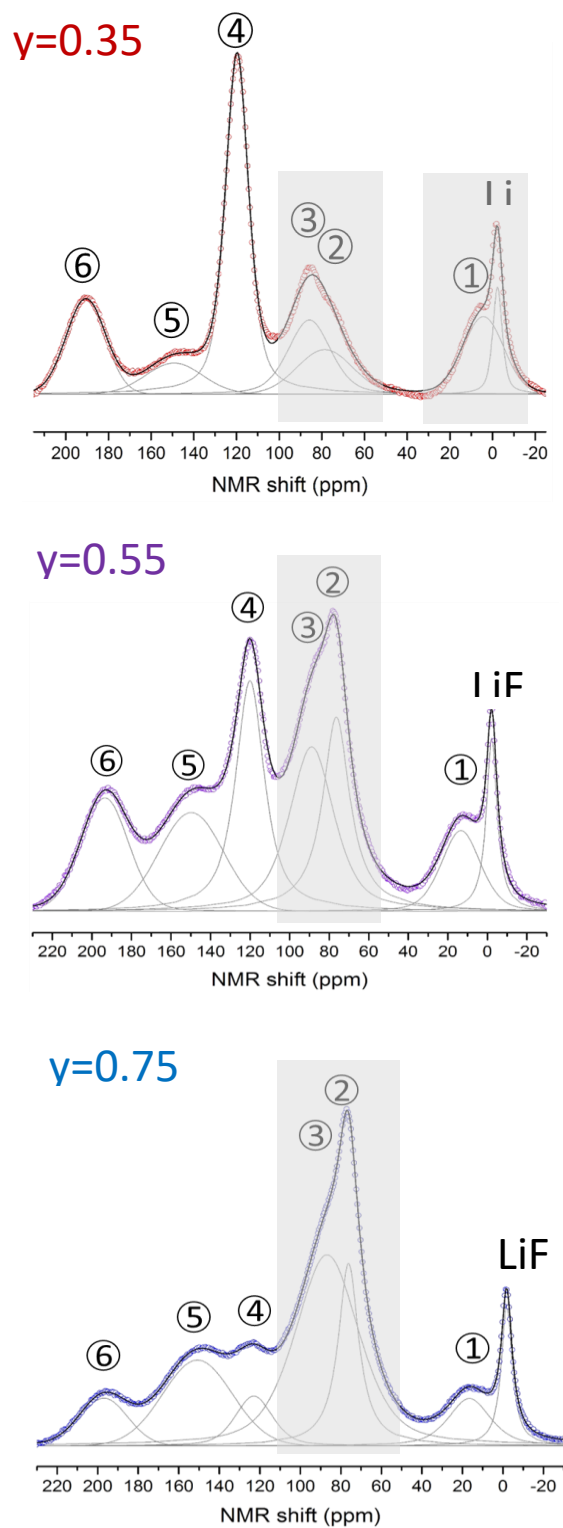


**Figure S3:** Tentative decomposition of the 1D  $^7\text{Li}$  MAS NMR spectra of the three intermediate  $\text{LiVPO}_4\text{F}_{1-y}\text{O}_y$  phases with  $y = 0.35, 0.55, 0.75$  using 6 contributions with a pseudo voigt lineshape in addition to the LiF contribution around 0ppm. Note that especially in the grey regions with strong overlap, more contributions could have been considered.

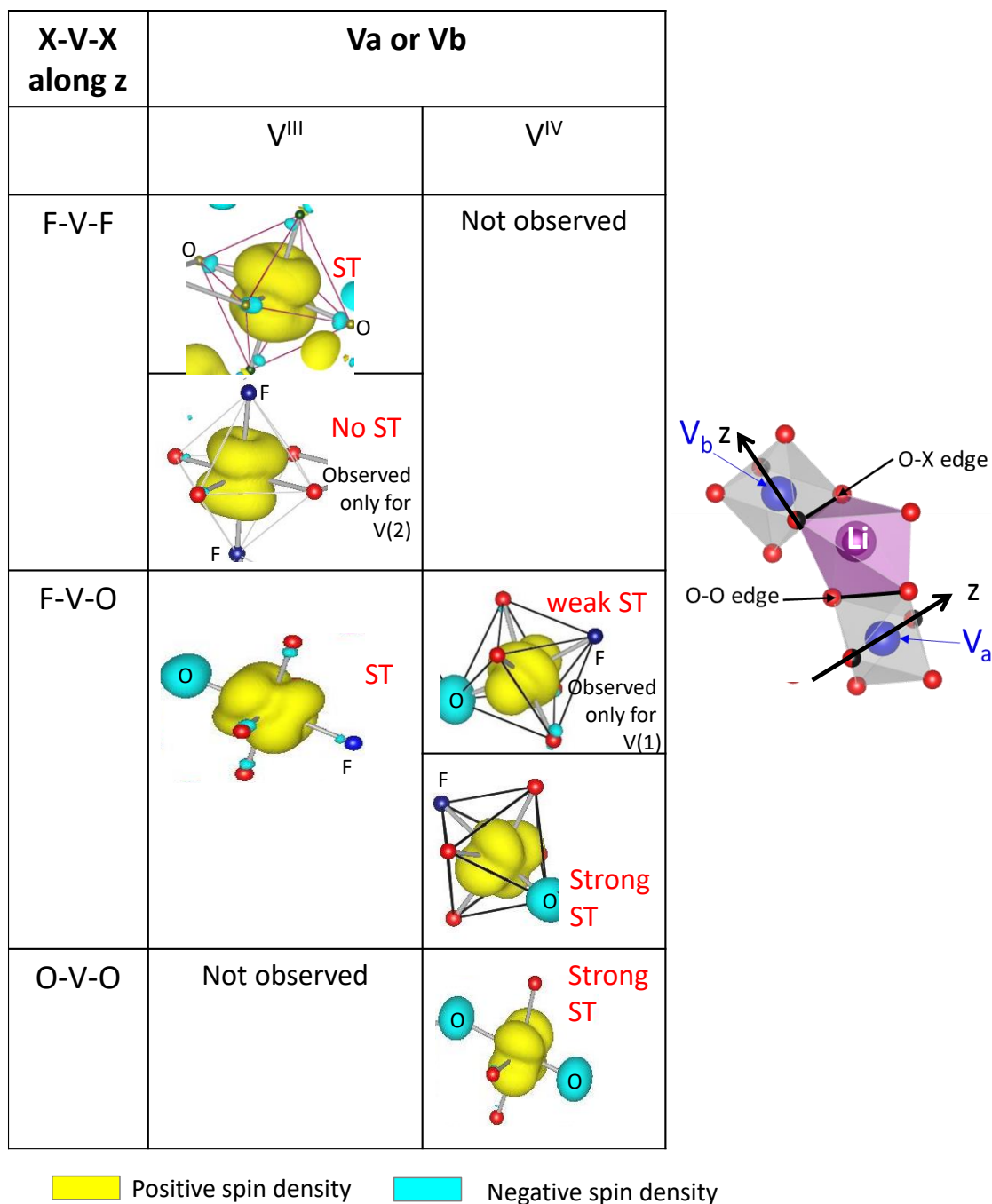


**Figure S4:** Spin density maps around V ions depending on their  $\text{VO}_4\text{X}_2$  environment typically calculated for  $\text{LiVPO}_4(\text{O},\text{F})$  model phases and their corresponding oxidation states  $\text{V}^{\text{III}}$  or  $\text{V}^{\text{IV}}$ . From the Li environment on the left, the expected magnitude of spin transfer from V to Li, relative to the spin transfer observed in  $\text{LiV}^{\text{III}}\text{PO}_4\text{F}$ , is deduced. ST = similar spin transfer, weak ST = weaker spin transfer, strong ST = larger spin transfer and no ST = almost no spin transfer.

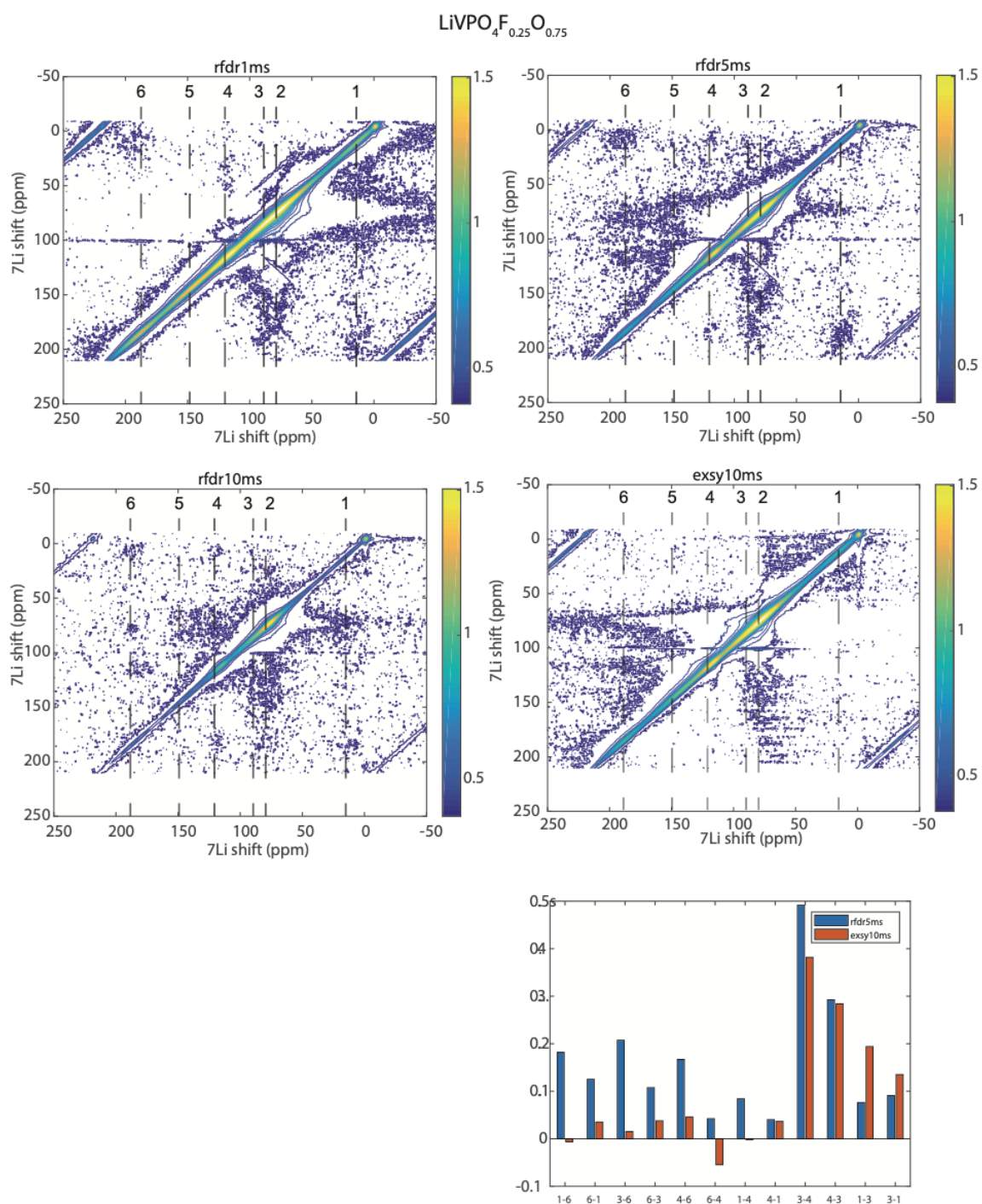


**Figure S5:**  ${}^7\text{Li}$ - ${}^7\text{Li}$  fp-RFDR correlation spectra with a mixing time of 1, 5 and 10 ms for  $\text{LiVPO}_4\text{F}_{0.25}\text{O}_{0.75}$ , with the  ${}^7\text{Li}$ - ${}^7\text{Li}$  EXSY correlation spectrum acquired in the same conditions with a mixing time of 10 ms. The cross peak areas are compared for the RFDR (5ms) and the EXSY at the bottom tight.

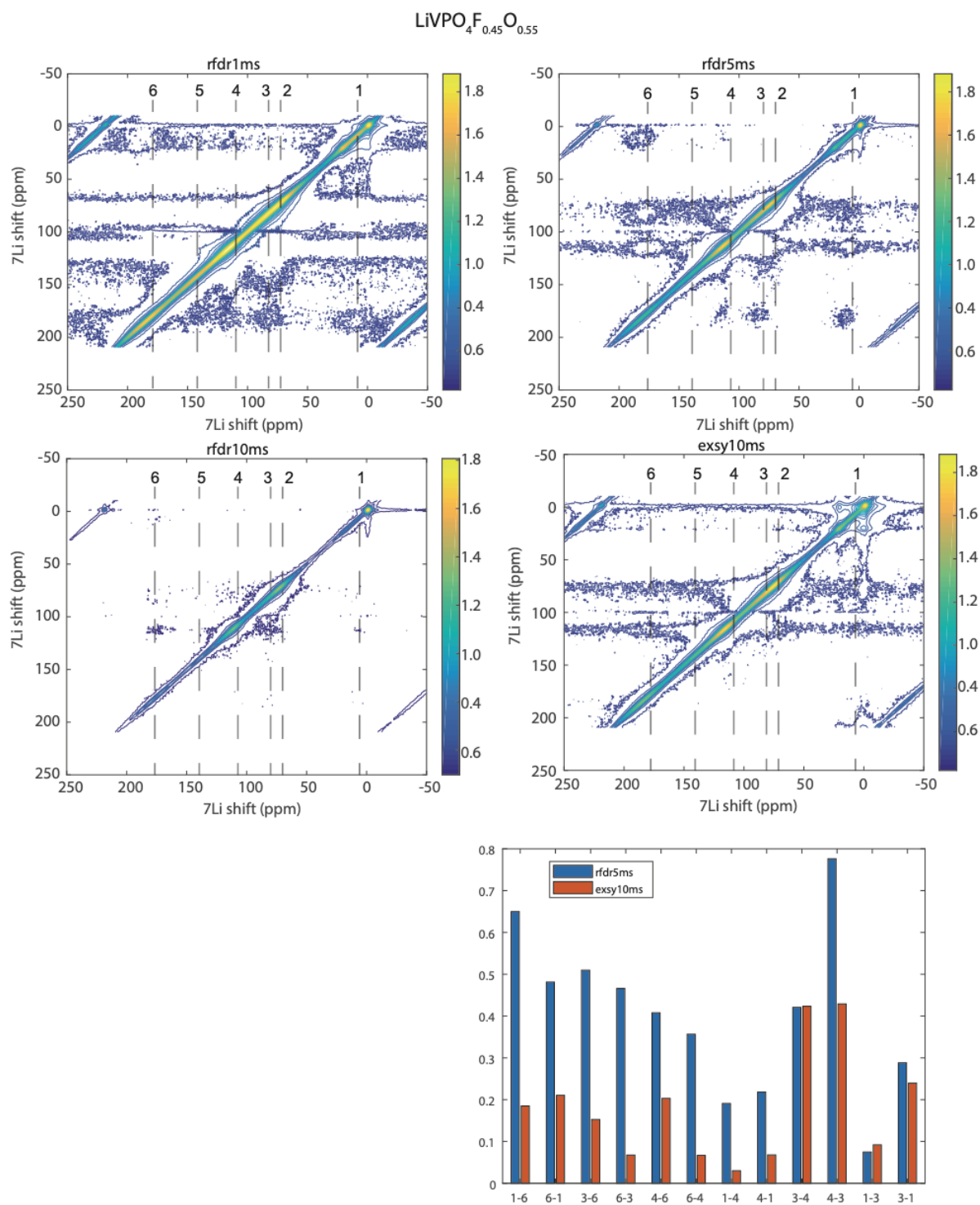


**Figure S6:**  ${}^7\text{Li}$ - ${}^7\text{Li}$  fp-RFDR correlation spectra with a mixing time of 1, 5 and 10 ms for  $\text{LiVPO}_4\text{F}_{0.45}\text{O}_{0.55}$ , with the  ${}^7\text{Li}$ - ${}^7\text{Li}$  EXSY correlation spectrum acquired in the same conditions with a mixing time of 10 ms. The cross peak areas are compared for the RFDR (5ms) and the EXSY at the bottom right.

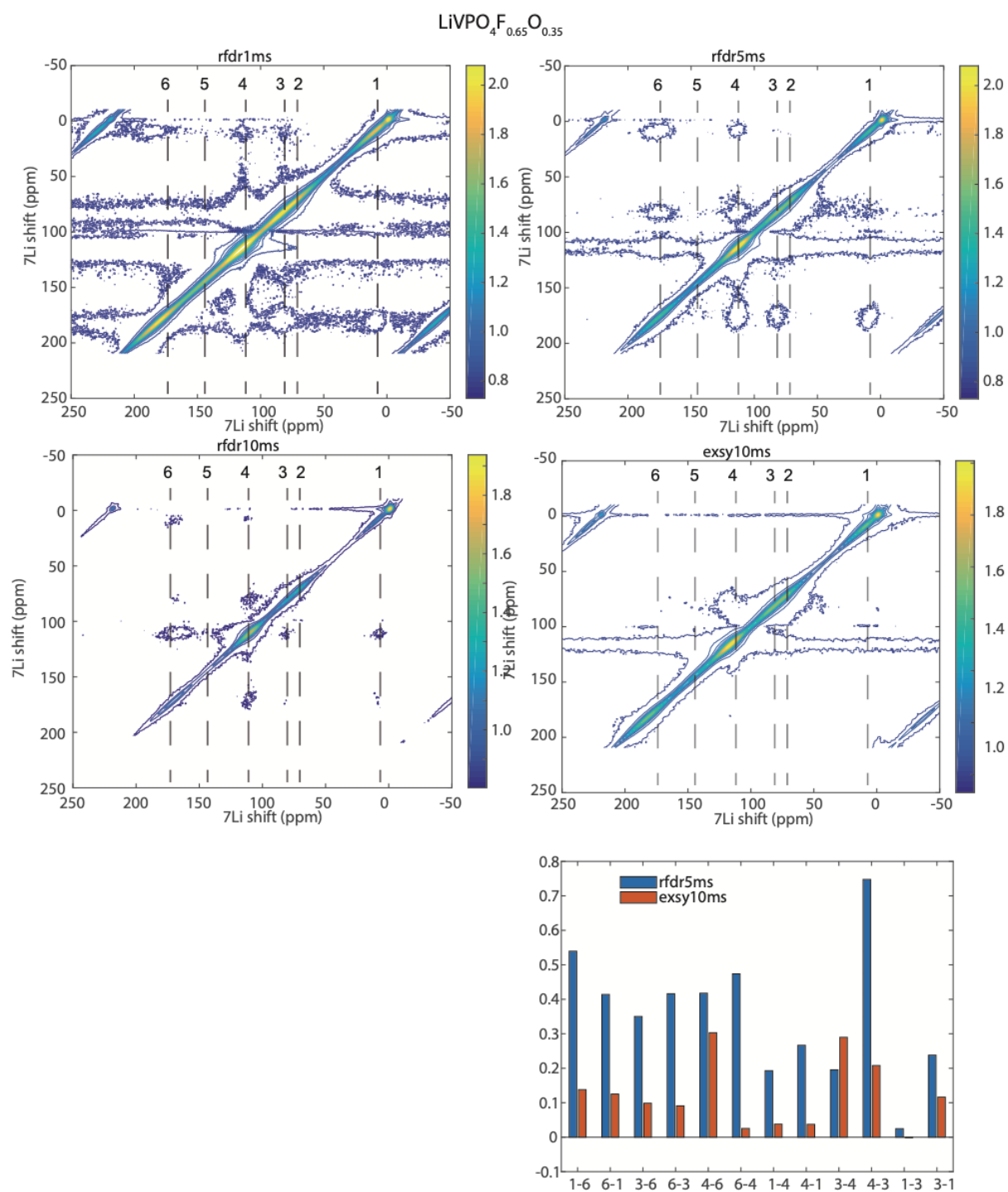


**Figure S7:**  ${}^7\text{Li}$ - ${}^7\text{Li}$  fp-RFDR correlation spectra with a mixing time of 1, 5 and 10 ms for  $\text{LiVPO}_4\text{F}_{0.65}\text{O}_{0.35}$ , with the  ${}^7\text{Li}$ - ${}^7\text{Li}$  EXSY correlation spectrum acquired in the same conditions with a mixing time of 10 ms. The cross peak areas are compared for the RFDR (5ms) and the EXSY at the bottom right.



## References

- [1] T. Bamine, T. E. Boivin, F. Boucher, R. Messinger, E. Salager, M. Deschamps, C. Masquelier, L. Croguennec, M. Ménétrier, D. Carlier, *J. Phys. Chem. C* **2017**, *121* (6), 3219–3227.
- [2] L-H-B Nguyen, P. Sanz Camacho, T. Broux, J. Olchowka, C. Masquelier, L. Croguennec, D. Carlier, *Chem. Mater.* **2019**, *31*(23), 9759-9768. L-H-B Nguyen, P. Sanz Camacho, T. Broux, J. Olchowka, C. Masquelier, L. Croguennec, D. Carlier, *Chem. Mater.* **2019**, *31*(23), 9759-9768.
- [3] D. Carlier, M. Ménétrier, C. Delmas *J. Phys. Chem. C*, **2010**, *114*, 4749-4755.
- [4] A. Castets, D. Carlier, Y. Zhang, F. Boucher, N. Marx, L. Croguennec, M. Ménétrier, *J. Phys. Chem. C*, **2011**, *115*, 16234-16241.